

# Dewetting of polymethyl methacrylate on the patterned elastomer substrate by solvent vapor treatment

Rubo Xing<sup>a,b</sup>, Chunxia Luo<sup>a,b</sup>, Zhe Wang<sup>a,b</sup>, Yanchun Han<sup>a,b,\*</sup>

<sup>a</sup> State Key Laboratory of Polymer Physics and Chemistry, Changchun Institute of Applied Chemistry, Chinese Academy of Sciences, 5625 Renmin Street, Changchun 130022, People's Republic of China

<sup>b</sup> Graduate University of the Chinese Academy of Sciences, 5625 Renmin Street, Changchun 130022, People's Republic of China

Received 21 July 2006; received in revised form 3 April 2007; accepted 11 April 2007

Available online 24 April 2007

## Abstract

The dewetting evolution process of polymethyl methacrylate (PMMA) film on the flat and prepatterned polydimethylsiloxane (PDMS) substrates (with square microwells) by the saturated solvent of methyl ethyl ketone (MEK) treatment has been investigated at room temperature by the optical microscope (OM) and atomic force microscope (AFM). The final dewetting on the flat PDMS substrate led to polygonal liquid droplets, similar to that by temperature annealing. However, on the patterned PDMS substrate, depending on the microwells' structure of PDMS substrate and defect positions that initiated the rupture and dewetting of PMMA, two different kinds of dewetting phenomena, one initiated around the edge of the microwells and another initiated outside the microwells, were observed. The forming mechanism of these two different dewetting phenomena has been discussed. The microwells were filled with liquid droplets of PMMA after dewetting due to the formation of fingers caused by the pinning of the three-phase-line at the edge of the microwells and their rupture.

© 2007 Elsevier Ltd. All rights reserved.

*Keywords:* Dewetting; Elastomer; Patterning

## 1. Introduction

Dewetting of thin polymer film is of great significance because of its potential and important engineering applications [1–4]. Especially, in recent years, morphology and its evolution process of controlled dewetting of thin polymer films have aroused more and more theoretical and experimental study interests because of its patterning ability in micro- and nanometer scales [5–22].

In this area, an important route to realize the surface patterning is the dewetting of thin polymer films on the substrate with physical or chemical heterogeneous pattern. Rehse et al. [5] investigated in detail the dewetting process of thin polystyrene

(PS) films of varying molecular weight on the regularly grooved silicon substrate without chemical heterogeneity. The PS films dewet the substrate and formed nanometer scale PS channels filling the groove of the substrate when the films' thickness is below a critical value. Higgins and Jones [6] reported an anisotropic spinodal dewetting of polymer film on rough surface by simply rubbing the substrate. Orientation morphology of dewetted film aligned with the substrate pattern was observed. By using a nanoscope grooved silicon substrate with alternating Au and silicon oxide stripes, Rockford et al. [7] researched the dewetting of thin PS films. They showed that the substrate could act as a template to control the dewetting.

Using surface energy pattern, such as chemical heterogeneous pattern, as a template to control dewetting is also a valid route to realize the pattern replication of surface pattern. Meyer and Braun [8] generated ordered polymer drops on a chemically modified surface by microcontact printing. It was reported that the holes were formed exclusively on the hydrophilic microprinted areas due to poor wettability of the

\* Corresponding author. State Key Laboratory of Polymer Physics and Chemistry, Changchun Institute of Applied Chemistry, Chinese Academy of Sciences, 5625 Renmin Street, Changchun 130022, People's Republic of China. Tel.: +86 431 85262175; fax: +86 431 85262126.

E-mail address: [yhan@ciac.jl.cn](mailto:yhan@ciac.jl.cn) (Y. Han).

polymer film. Sharma et al. [9] investigated systematically the morphology evolution process of dewetting of dry polymer films deposited on chemically patterned substrate based on 3D nonlinear simulations and found that there must be some coupling between the characteristic length scale of dewetting and the substrate surface pattern. They predicted the possibility of patterning surface on patterned substrate and showed that ideal template occurred only when the period of the substrate pattern was greater than the spinodal wavelength but less than an upper transition length where dewetting was initiated on the boundary of the patterns on the substrate. Karim et al. [10] utilized the chemically patterned substrates with arrays of progressively narrower stripes (1–15  $\mu\text{m}$ ) to investigate the influence of pattern size on the morphology of ultrathin dewetting polystyrene films. Dewetting patterns were correlated to the substrate pattern period leading to the formation of droplet arrays. The measurements confirm recent numerical simulations by Kargupta and Sharma [9] of the existence of upper and lower cutoff scales for pattern recognition of a dewetting fluid.

Taking into account another example, Lee et al. [18] reported the confined and anisotropic dewetting of polymer films that took place when a thin polystyrene film confined by polydimethylsiloxane walls dewet on a silicon substrate at the temperature above its glass transition temperature, resulting in the formation of a regular structure inside and outside the confinement. There are also some other methods that have been used to realize the polymer patterning through dewetting process of thin polymer films.

Motivated by the research work above, we investigated the dewetting evolution process of PMMA film on the flat and prepatterned PDMS substrates in the saturated solvent of methyl ethyl ketone (MEK) at room temperature. The patterned PDMS substrate has well defined square microwells without chemical heterogeneity. The dewetting on the flat PDMS substrate led to form polygonal liquid droplets, similar to that by temperature annealing of thin polymer films on homogeneous substrate. However, on the patterned PDMS substrate, depending on the microwells' structure of PDMS substrate and defect positions that initiated the rupture and dewetting of PMMA films, two different kinds of dewetting phenomena, one initiated around the edge of the microwells and another initiated outside the microwells, were observed. A convincing mechanism has been provided to explain the formation of these different phenomena. These dewetting processes left polymer dots in every microwell and formed the pattern of the polymer films accorded with the pattern of the PDMS substrate at room temperature. This technique could be used to realize the patterning of functional polymer films through combination of microtransfer printing [24] to fabricate the organic electronic devices such as polymer light-emitting diodes and polymer field-effect transistors.

## 2. Experimental

### 2.1. Fabrication of prepatterned PDMS substrate

Silicon wafer with ordered square mesas (area  $20\ \mu\text{m} \times 20\ \mu\text{m}$ , height 520 nm, etched by photolithography and RIE)

and glass slides were both cleaned by the ultrasonic treatment in acetone and alcohol for 10 min, respectively, and then blown dry with nitrogen. The polydimethylsiloxane (PDMS) elastomer is Sylgard 184 obtained from Dow Curing. It was supplied as a two-part kit: a liquid silicon base (i.e. a vinyl-terminated PDMS) and a catalyst or curing agent (i.e. a mixture of a platinum complex and copolymer of methylhydrosiloxane and dimethylsiloxane). In the experiment, the liquid silicon base was mixed with curing agent at a mix ratio of 10:1 (w/w). Then the mixture was cast on the patterned silicon wafer and heated at 65 °C for 4 h after covered with a piece of clean glass. The mixed liquid mixture became a solid, cross-linked elastomer via the hydrosilylation reaction between vinyl ( $\text{SiCH}=\text{CH}_2$ ) groups and hydrosilane ( $\text{Si}-\text{H}$ ) groups. Subsequently, carefully peeled off from the silicon wafer, the elastomer PDMS (still stickup with the glass) with the replicas of the structure of the patterned silicon wafer was formed. Then, the elastomer sticking on the clean glass sheet acted as the substrate in the dewetting investigation. The flat PDMS substrate can be fabricated from the same method using the flat silicon wafer instead of the patterned silicon wafer.

### 2.2. Sample preparation

Polymethyl methacrylate (PMMA) (average molecular weight ( $M_w$ ), 233,000 g/mol) was purchased from Aldrich Chem. Co. The PMMA film was deposited onto the clean flat and prepatterned PDMS substrates by spin coating (1500 rpm) from a methyl ethyl ketone (MEK) solvent (boiling point:  $T_b = 79.57\ \text{°C}$ ; melting point:  $T_m = -85.9\ \text{°C}$  [26]) solution (3.0 wt% polymer/MEK solutions were filtered through 0.22  $\mu\text{m}$  PTFE filters before spin coating). To remove the residual solvent, both of the films were kept in vacuum at 55 °C overnight. The PMMA film deposited on the flat PDMS substrate was detected by spectroscopic ellipsometry (SE) and the film thickness was of 110 nm. The glass transition temperature of the bulk PMMA was 105 °C determined by means of differential scanning calorimeter (DSC).

### 2.3. Solvent vapor annealing

First, the PMMA films on the flat and patterned PDMS substrates were placed on a hot stage at 160 °C to observe its dewetting behavior. Then, the PMMA film on the flat and patterned PDMS substrates was placed in a chamber full of saturated vapor of MEK (the pressure was about 100 mmHg at 25 °C [26]) at room temperature (about 26 °C) for different times. The morphology evolution processes of PMMA films were observed by polarized light microscope (PLM) (Leica Co., Type: THMSE600) with a digital CCD camera attachment. Atomic force microscope (AFM) (SPA300HV with an SPI3800 controller, Seiko Instruments Industry, Co., Ltd.) was also used to observe the dewetted pattern.

### 3. Results and discussion

#### 3.1. Dewetting of PMMA film on the flat PDMS substrate

Optical micrograph indicated that the PMMA films on the flat substrate were smooth and uniform when inspected immediately after spin coating. It is metastable because the interfacial energy between PDMS (surface free energy:  $21.6 \times 10^{-3} \text{ J m}^{-2}$ ) and PMMA (surface free energy:  $32.0 \times 10^{-3} \text{ J m}^{-2}$ ) is very large due to the weak affinity force between these two polymers. Thus, to PMMA film, the substrate is nonwetable, i.e., the film is just only a metastable one, which is not in the thermodynamic stability. If the PMMA film experiences the complicated and significant activation process of the frozen block chain of the glassy polymer, the metastable film on the nonwetable substrate would undergo the process, the so-called dewetting.

The films were then annealed at  $160^\circ\text{C}$  above the glass transition temperature of the PMMA ( $T_g = 105^\circ\text{C}$ ) to observe the dewetting process. Once annealed, the thin PMMA film ruptured and formed nucleated holes at early stage as shown in Fig. 1(a), followed by hole growth (Fig. 1(b)), coalescence (Fig. 1(c)) and finally formation of polygonal liquid droplets (Fig. 1(d)–(f)). It would be possible that the glass transition was activated by the solvent vapor annealing when the temperature was below the  $T_g$  [23]. Fig. 2 illustrates the dewetting process of PMMA film on the flat PDMS substrate placed in the saturated MEK solvent vapor at room temperature (about  $26^\circ\text{C}$ ) for a certain time. Three different stages can be distinguished. At the beginning of solvent annealing, the smooth films broke up at the position of heterogeneities (impurities or defects) in the film or on the substrate, resulting in circular holes (Fig. 2(a)). The holes then grew with the increase of the annealing time (Fig. 2(b)–(c)) and ribbons formed (Fig. 2(d)). The ribbons were unstable and decayed into droplets after certain time. Fig. 2(e) shows the polymer droplet after the solvent evaporation at the late stage of dewetting.

From the above description, it could be seen that, as a whole, the dewetting process of thin PMMA films on the flat PDMS substrate by solvent vapor annealing was similar to that annealed by heating. However, there also exist some differences, such as rupture position, density of holes and the scale of droplets. These differences might come from the thickness increase of thin PMMA films when it annealed at solvent vapor environment. In this condition thin PMMA films absorbed solvent vapor and were swollen. Because of the confinement of PDMS substrate thin PMMA films expanded in the vertical direction and caused the thickness increase. In a thicker film the rupture of the films became more difficult. Thus, only a few large defects could cause the rupture of the thin PMMA films and initiated the dewetting as shown in Fig. 2(b). Therefore, the rupture position and density of holes decreased in the solvent vapor annealing condition compared with that annealed by heating. It was certain that the density decrease of holes caused a larger amount of polymer aggregate to the ribbons. The larger amount of polymer and swelling made the diameter of the ribbons larger than the diameter of the ribbons in the heating annealing condition. From previous

works [2] the ribbons will decay via Rayleigh instability into droplets of size proportional to the diameter of the ribbons. So in the dewetting process of solvent vapor annealing the ribbons were difficult to rupture and decayed into very large droplets of materials as shown in Fig. 2(e).

#### 3.2. Dewetting on the prepatterned PDMS substrate

To investigate the effect of pattern of the substrate on dewetting processes, the prepatterned PDMS has been used as substrates. At first, the PMMA film on the patterned PDMS substrate was placed on a hot stage at  $160^\circ\text{C}$  to observe its dewetting behavior. Fig. 3 shows the optical micrographs of the dewetting process. The thin PMMA film ruptured at the defect positions and sidewalls of the microwells and formed nucleated holes as shown in Fig. 3(a). With the growth of the holes, all the rims receded at the inner and the outer of the microwells and inclined to form circular holes (Fig. 3(b)). The holes then grew with the increase of the annealing time and ribbons formed (Fig. 3(c)). The ribbons were unstable and decayed into droplets after certain time (Fig. 3(d)). Followed the receding of the rims, a slight pinning of the rims happened at the sidewalls of the microwells and formed thin fingers [25]. The fingers broken up finally and left small polymer dots at the inner and the outer of the microwells.

Then the dewetting process of thin PMMA films on the patterned PDMS substrate by solvent vapor annealing has also been investigated. Figs. 4 and 5 show the experimental results. Compared with the dewetting process of thin PMMA film on the patterned PDMS substrate by heating, only a few large defects caused the rupture of the thin PMMA films and initiated the dewetting, which are similar to the situation of dewetting processes on flat PDMS substrate by heating and solvent vapor annealing. But two different kinds of dewetting phenomena, one initiated around the edge of the microwells and another initiated outside the microwells, were observed on the prepatterned PDMS substrate as shown in Figs. 4 and 5, respectively.

For the dewetting initiated around the edge of the microwells, just like the dewetting process of the PMMA film on the flat PDMS substrate, the heterogeneities' nucleation growth dewetting was initiated around the edge of the microwells and a circle-like hole formed (Fig. 4(a)). The holes radius grew up to about  $200 \mu\text{m}$  after solvent annealing for 290 min (Fig. 4(b)). With the increase of the solvent vapor annealing time, the hole continued to grow and contacted with the adjacent holes as observed in Fig. 4(c). Finally, due to the Rayleigh instability of the long cylindrical masses, the PMMA ribbons eventually decayed into large droplets (Fig. 4(d)).

It was noteworthy that in the dewetting process, the PMMA mass selectively remained in each microwell instead of moving with the rims since the rims developed regular fingers and the fingers broke up and droplets left in the microwells. In our experiment, the growth of holes during dewetting was absolutely the receding process of the three-phase-line on the PDMS substrate with ordered square microwells (Fig. 4(e)). When the three-phase-line encountered the edge of the

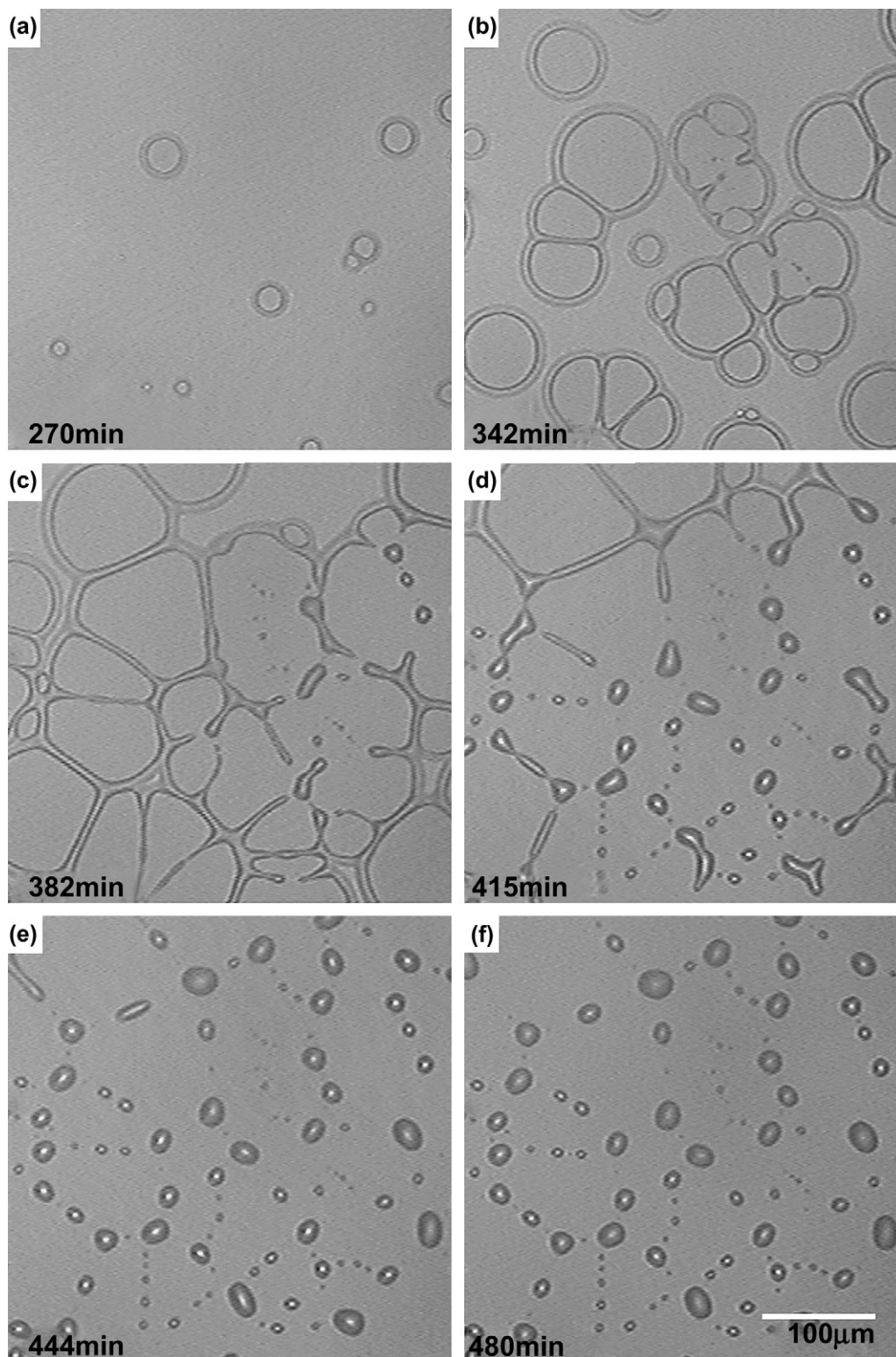


Fig. 1. Optical micrographs of the dewetting pattern of PMMA on the flat PDMS substrate at 160 °C above its glass transition temperature for different times: (a) 270 min; (b) 342 min; (c) 382 min; (d) 415 min; (e) 444 min; and (f) 480 min.

microwells, the sudden change of the surface morphology caused the increase of the contact angle and pinning of the three-phase-line on the edge of the microwells [25]. The local pinning of the three-phase-line, combined with the receding of the rims continuously, formed a finger from the position of

every microwell. Compared with the dewetting process of thin PMMA film on the patterned PDMS substrate by heating, thicker and regular fingers have formed at the edge of the microwells in the condition of solvent vapor annealing. This effective local pinning may come from the larger thickness of

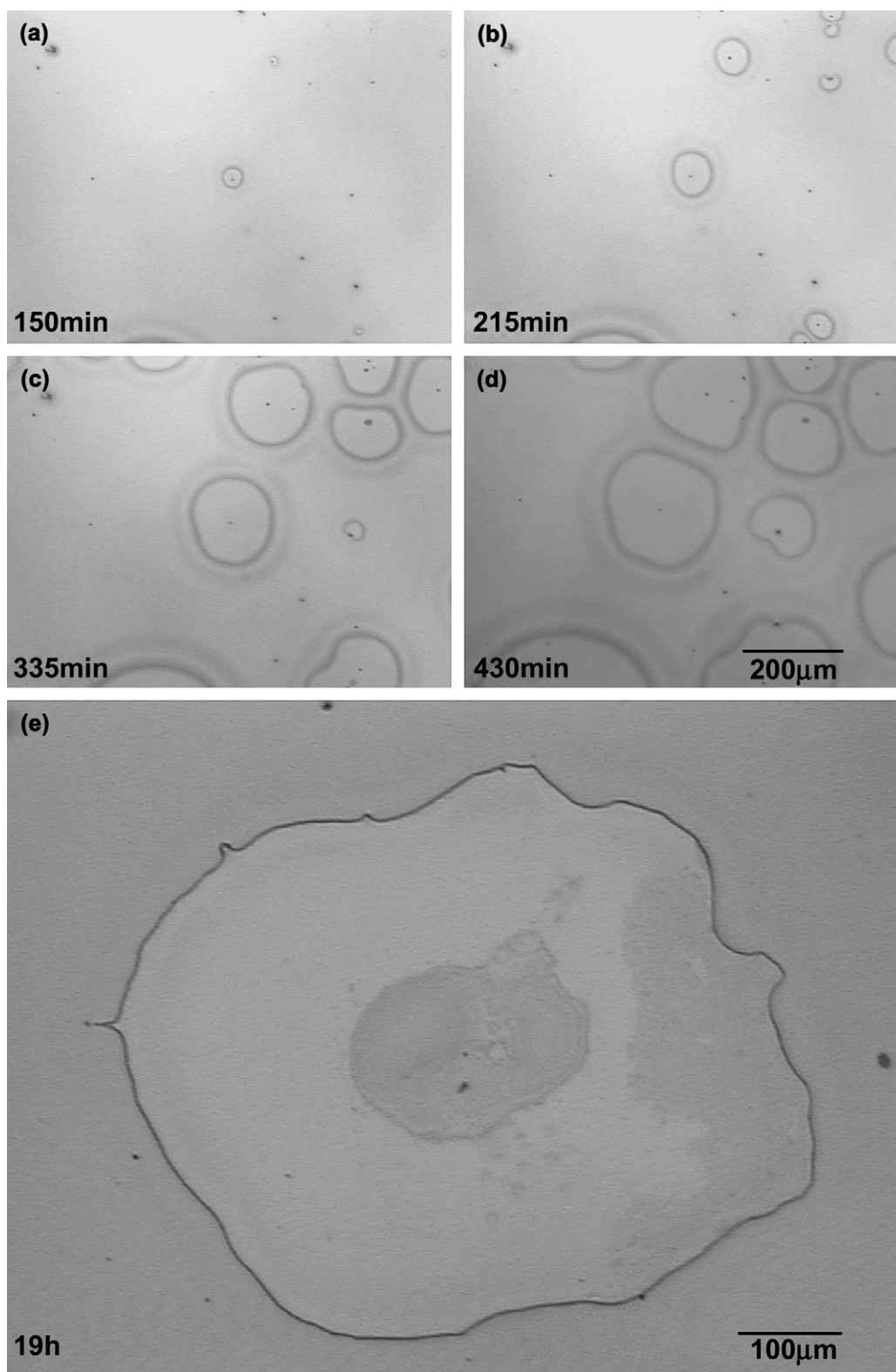


Fig. 2. Optical micrographs of the dewetting pattern of PMMA film on the flat PDMS substrate by the saturated vapor methyl ethyl ketone (MEK) treatment at room temperature (about 26 °C) for different times: (a) 150 min; (b) 215 min; (c) 335 min; and (d) 430 min. (e) The dewetted droplet of PMMA on the PDMS substrate.

the PMMA film because of the swelling of the polymer materials, which could also be seen at the end stage of the dewetting process of thin PMMA film on the patterned PDMS substrate by heating (Fig. 3(d)).

The finger began to bud from the edge of each microwell. With the following receding of the three-phase-line, as shown in the Fig. 4(e), the finger had the tendency to move with the receding three-phase-line. The surface tension force made the

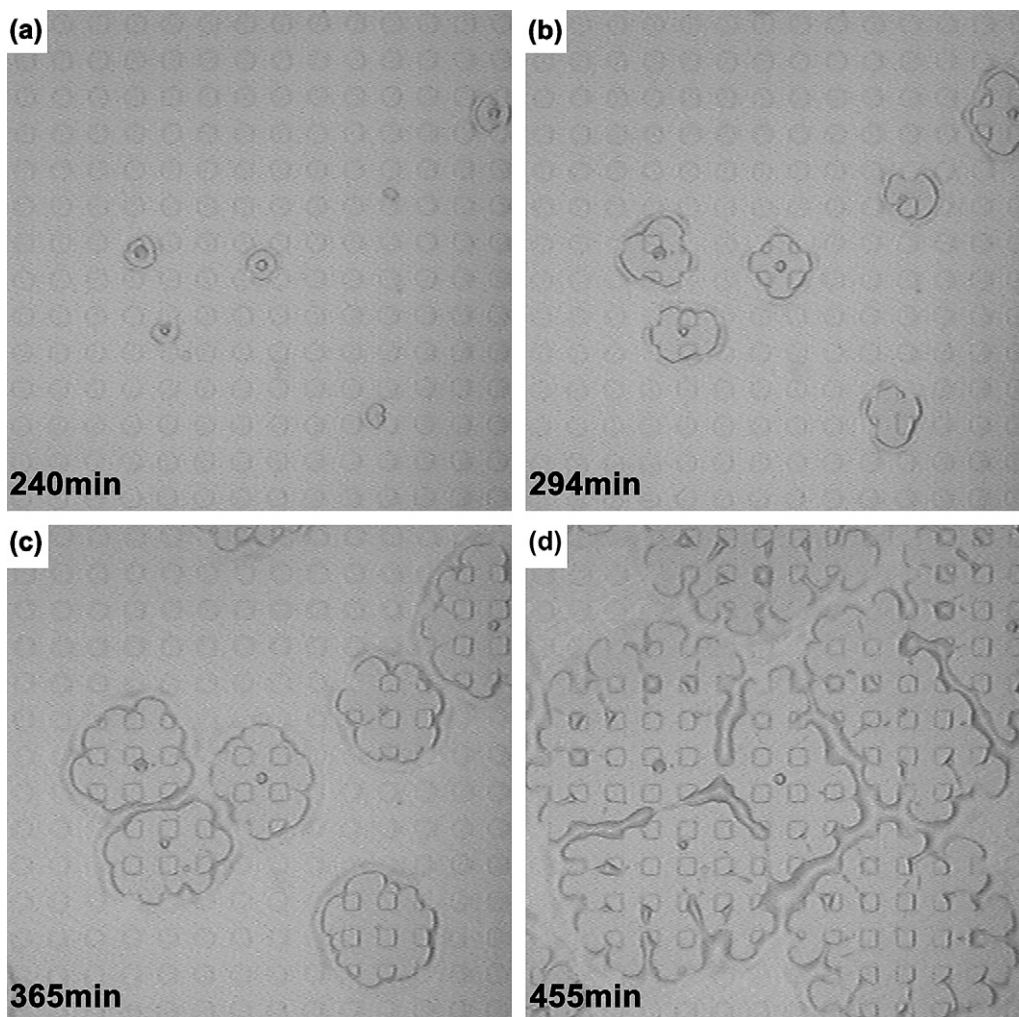


Fig. 3. Optical micrographs of the dewetting pattern of PMMA on the patterned PDMS substrate at 160 °C above its glass transition temperature for different times: (a) 240 min; (b) 294 min; (c) 365 min; and (d) 455 min.

three-phase-line recede continuously. The finger grew longer and the bottleneck formed due to the second Rayleigh instability as seen in Fig. 4(e). Finally, the bottleneck became smaller and smaller till the breakup of the finger at the neck. Therefore, the liquid droplet of PMMA stayed in the microwells (Fig. 4(e)). This process repeated again and again and droplets remained in the microwells until the rims of adjacent holes coalescence each other.

Another kind of dewetting phenomenon is described in Fig. 5. The dewetting was initiated outside the microwells and formed holes. The holes grew just like the star with four tines. In this dewetting process, fingers were also observed. The droplets stayed in microwells similar to the dewetting process described above. The rims of the polymer holes were sawtooth-like because of the formation of fingers.

What determined the two different kinds of dewetting phenomena? Compared to the dewetting phenomena of PMMA films on the flat PDMS substrate by solvent vapor annealing and on the patterned PDMS substrate by heating, it was possible that the solvent vapor annealing, the microwells' structure of PDMS substrate and the defect positions that initiated the

rupture and dewetting of thin polymer films were responsible for it.

The PDMS substrate with microwells structure and the solvent vapor annealing could cause the anisotropic of rims' receding speed in the dewetting process which might come from the local pinning of the three-phase-line and the swelling of the PDMS substrate. First, the local pinning of the rims at the edges of the microwells caused that the rims' receding speed at the region of microwells was higher than that of the smooth regions between the microwells. On the other hand, from Fig. 4(e) it is clear that the surface of the PMMA films was smooth in the dewetting process by solvent vapor annealing. At the same time the swelling of the PDMS substrate could make the center of the smooth regions between the microwells higher because of the anisotropic swelling of the patterned PDMS substrate. These factors caused the facts that the thickness of the swelling polymer films was smaller in the center of the smooth regions between the microwells, and the receding speed of rims was higher in the center of the smooth regions compared with the receding speed in the edge of these regions. Combined the local pinning of three-phase-line at the

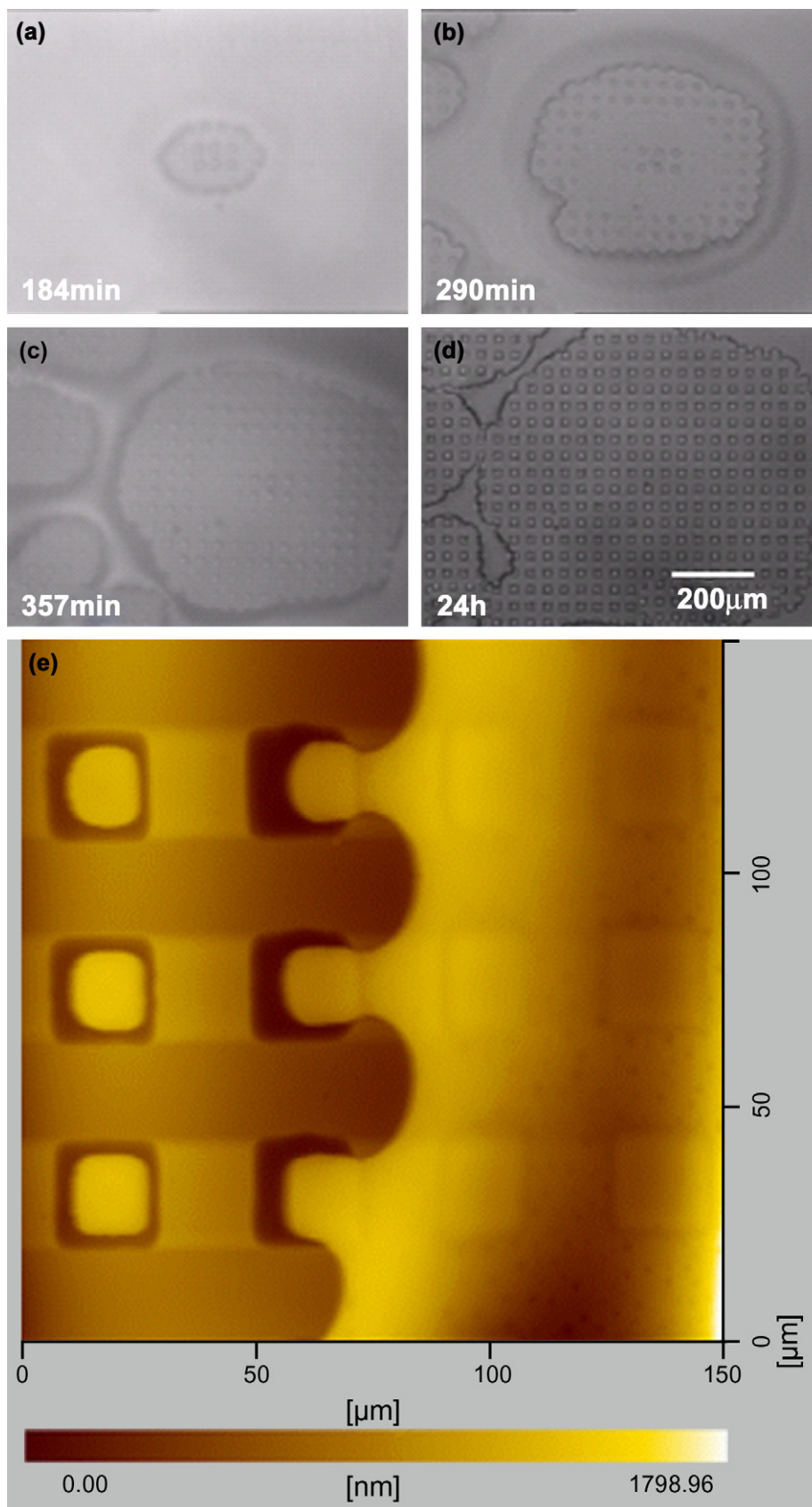


Fig. 4. Optical micrographs of the circular holes' progress during the dewetting evolution processes of PMMA film initiated at the edge of the square microwells by the saturated methyl ethyl ketone (MEK) vapor treatment at room temperature for different times: (a) 184 min; (b) 290 min; (c) 357 min; and (d) 24 h. The white bar is 200 μm. (e) The AFM image of the edge of the dewetted pattern on the PDMS substrate.

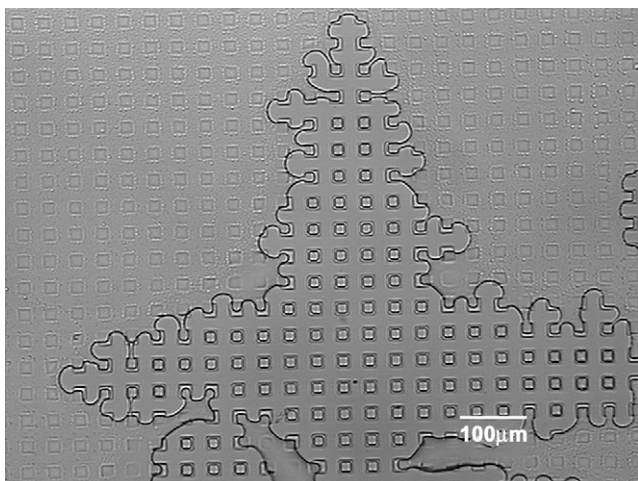


Fig. 5. Optical micrograph of the star-like hole of PMMA film during the dewetting of PMMA film initiated outside the square microwells on the PDMS substrate by the saturated vapor methyl ethyl ketone (MEK) treatment at room temperature.

edge of microwells, rims with arc configuration between the microwells have formed. The phenomenon could be seen clearly in the Fig. 5.

Combined the anisotropic of rims' receding speed with the rupture positions of the dewetted polymer films, the different phenomena of dewetting process can be explained. Fig. 6 shows the initial dewetting process of thin PMMA film on the prepatterned by solvent vapor annealing at room temperature. Based on the experimental result, Fig. 7 gives a detailed drawing about the ideal dewetting process of the thin PMMA films on the PDMS substrate with microwells' morphology by MEK vapor annealing. When the dewetting was initiated around the edge of the microwells (Fig. 7(a)), the dewetting onset occurred around the microwells and the holes grew symmetrically. This situation could lead to the circular-like holes growth. In the second situation (Fig. 7(b)), the dewetting was initiated outside the microwells. The dewetting speed in the smooth regions was higher, so the rims were driven along the smooth channels and extended to a star-like hole with four tines.

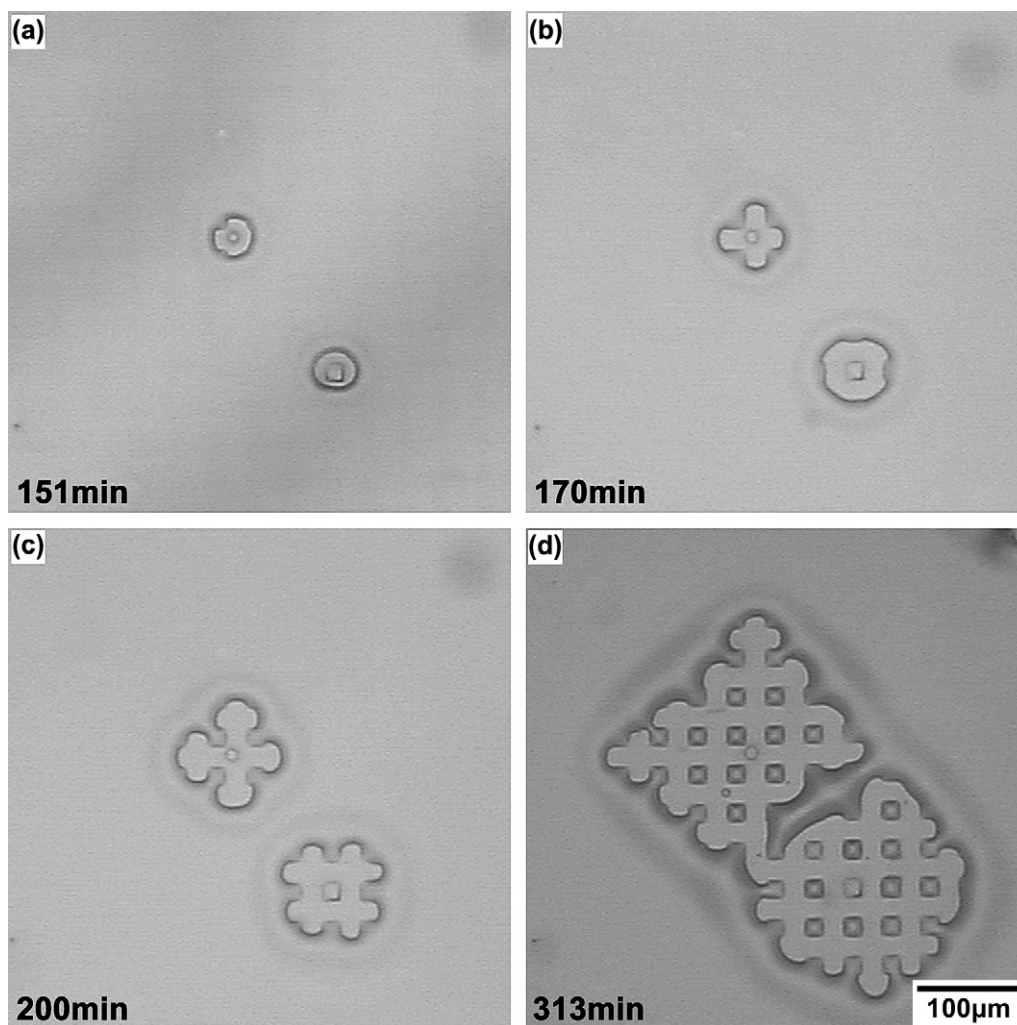


Fig. 6. Optical micrographs of the initial dewetting process of PMMA films on the prepatterned PDMS substrate by solvent vapor annealing at room temperature for different times: (a) 151 min, (b) 170 min, (c) 200 min, and (d) 313 min.



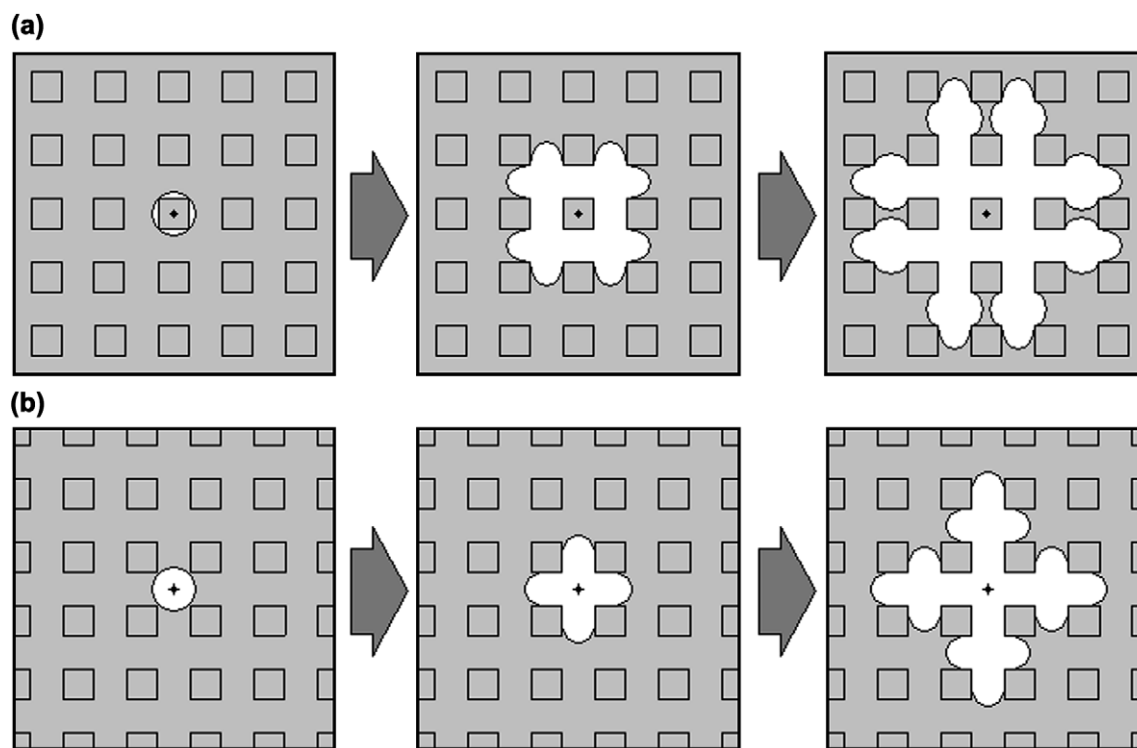


Fig. 7. Formation processes of the different dewetting holes. The black dot in the center of the square represents the dewetting initiation position. (a) The formation process of the circle dewetting hole. (b) The formation process of the tetragon-like dewetting hole.

#### 4. Conclusion

The dewetting evolution process of PMMA film on the flat and prepatterned PDMS substrates have been investigated in the saturated solvent vapor of methyl ethyl ketone (MEK) at room temperature. Similar to annealing by heating, once annealed by solvent vapor, the thin PMMA film exhibited a typical pattern of dewetting initiated by nucleated holes, followed by holes' growth and coalescence and finally formation of polygonal liquid droplets. However, depending on the defect positions and the anisotropic receding speed of rims caused by the local pinning of the three-phase-line and the PDMS substrate swollen by solvent, two different kinds of the dewetting process were observed on the patterned PDMS substrate. The microwells were filled with liquid droplets of PMMA after dewetting due to the formation of fingers caused by the local pinning of the three-phase-line during the receding of the three-phase-line.

#### Acknowledgment

This work is subsidized by the National Natural Science Foundation of China (20621401, 50403007).

#### References

- [1] Reiter G. *Phys Rev Lett* 1992;68:75.
- [2] Reiter G. *Langmuir* 1993;9:1344.
- [3] Xie R, Karim A, Douglas JF, Han CC, Weiss RA. *Phys Rev Lett* 1998;81:1251.
- [4] Seemann R, Herminghaus S, Jacobs K. *Phys Rev Lett* 2001;86:5534.
- [5] Rehse N, Wang C, Hund M, Geoghegan M, Magerle R, Krausch G. *Eur Phys J E* 2001;4:69.
- [6] Higgins AM, Jones RAL. *Nature* 1999;404:476.
- [7] Rockford L, Liu Y, Mansky PT, Russell P, Yoon M, Mochrie SGJ. *Phys Rev Lett* 1999;82:2602.
- [8] Meyer E, Braun HG. *Macromol Mater Eng* 2000;276(3–4):44.
- [9] (a) Sharma A, Reiter G. *J Colloid Interface Sci* 1996;178:383; (b) Sharma A. *Phys Rev Lett* 1998;81:3463; (c) Kargupta K, Sharma A. *Phys Rev Lett* 2001;86:4536; (d) Kargupta K, Sharma A. *Langmuir* 2003;19:5153; (e) Reiter G, Khanna R, Sharma A. *J Phys Condens Mater* 2003; 15:S331; (f) Kargupta K, Sharma A. *Langmuir* 2002;18:1893; (g) Kargupta K, Sharma A. *J Chem Phys* 2002;116:3042; (h) Kargupta K, Konnur R, Sharma A. *Langmuir* 2001;17:1294; (i) Kargupta K, Konnur R, Sharma A. *Langmuir* 2000;16:10243; (j) Konnur R, Kargupta K, Sharma A. *Phys Rev Lett* 2000;84:931.
- [10] Sehgal A, Ferreiro V, Douglas JF, Amis EJ, Karim A. *Langmuir* 2002; 18:7041.
- [11] Seemann R, Herminghaus S, Jacobs K. *J Phys Condens Mater* 2001; 13(21):4925.
- [12] Lu G, Li W, Yao JM, Zhang G, Yang B, Shen JC. *Adv Mater* 2002; 14:1049.
- [13] Zhang ZX, Wang Z, Xing RB, Han YC. *Surf Sci* 2003;539(1–3):129.
- [14] Lenz P, Lipowsky R. *Phys Rev Lett* 1998;80:1920.
- [15] Gau H, Herminghaus S, Lenz P, Lipowsky R. *Science* 1999;283:46.
- [16] Lipowsky R. *Curr Opin Colloid Interface Sci* 2001;6(1):40.
- [17] Gleiche M, Chi LF, Fuchs H. *Nature* 2000;403:173.
- [18] (a) Suh KY, Park J, Lee HH. *J Chem Phys* 2002;116:7714; (b) Suh KY, Lee HH. *Adv Funct Mater* 2002;12(6–7):405; (c) Suh KY, Lee HH. *J Chem Phys* 2001;115:8204.

- [19] Vermaa R, Sharma A, Banerjee I, Kargupta K. *J Colloid Interface Sci* 2006;296(1):220.
- [20] Kim YS, Lee HH. *Adv Mater* 2003;15:332.
- [21] Zhang XY, Xie FC, Tsui OKC. *Polymer* 2005;46:8416.
- [22] Lin ZQ, Kerle T, Russell TP. *Macromolecules* 2002;35:6255.
- [23] Leibler L, Sekimoto K. *Macromolecules* 1993;26:6937.
- [24] Luan SF, Cheng ZY, Xing RB, Wang Z, Yu XH, Han YC. *J Appl Phys* 2005;97:186102.
- [25] Ondarcuhu T, Piednoir A. *Nano Lett* 2005;5:1744.
- [26] *Solvents Guide*. 2nd ed., New York; 1963.